EXACT CALCULATION OF THE SCATTERING PROPERTIES OF OLIVINE IN A SALT MATRIX: APPLICATION TO MARS AND TROJAN ASTEROIDS. T. D. Glotch[1], J. A. Arnold[1], M. J. Wolff[2], and P. G. Lucey[3], [1]Department of Geosciences, Stony Brook University, tglotch@notes.cc.sunysb.edu, [2]Space Science Institute, [3]Hawaii Institute of Geophysics and Planetology, University of Hawaii.

Introduction: Current popular radiative transfer (RT)-based models [1,2] make the intrinsic assumption that individual particles are sufficiently well separated such that their interactions with the propagating electromagnetic fields take place in the "far-field", where one finds a significant simplification of the electrodynamical equations (and hence a reduced numerical burden) [see recent reviews by 3-4]. While these concepts have been understood for some time, the ability to solve generally for the scattered field in the presence of a cluster of particles has only been possible for the past ~15 years. Even then, it has been only in the last several years that such computations have become actually practical for more than a few particles.

In this work, we use a scattering code based on the direct computation of solutions to Maxwell's equations to exactly calculate the scattering properties of clusters of closely-packed spherical particles of forsteritic olivine and halite. A companion abstract uses the same approach to calculate the scattering properties of finely particulate quartz [5].

Understanding the scattering properties of silicates in a transparent salt matrix is relevant to remote sensing studies of Mars and asteroids. On Mars, mixtures of halide salts and silicates have been suggested to occur in some Noachian terrains due to their unique thermal infrared (TIR) and visible-near-infrared (VNIR) spectral properties [6-8]. Halide salts have also been proposed to cover the surfaces of Trojan asteroids, with scattering models suggesting the presence of a few percent olivine and a strong absorber such as nanophase iron or carbon dispersed throughout a transparent matrix [9].

Methods: We make use of the publicly available Multiple Sphere T Matrix (MSTM) code developed by D. Mackowski (http://eng.auburn.edu/users/dmckwski/scatcodes/) to calculate the scattering properties of clusters containing spherical particles [10]. Calculations at each wavelength were performed on the Brookhaven National Laboratory Blue Gene/P supercomputer. The basic code input is a sphere position file that describes the positions, sizes, and optical constants of the spheres in the cluster. We used two separate sphere cluster geometries to test the effects of olivine concentration and sphere packing on the resulting emissivity spectra. The first input (Case 1) defined a cluster of randomly distributed 2 μm diameter spheres with a packing efficiency (volume occupied by spheres/total volume) of ~30% and 1% olivine abundance. The second input (Case 2) defined a cluster of 377 cubic close packed 4 μm diameter spheres with a packing efficiency of ~74% and 1.9% olivine abundance. The configuration of this cluster of spheres is shown in Figure 1.

Outputs of the model at each wavelength include the normalized scattering phase function and the total extinction and scattering efficiencies (Q_{ext} and Q_{scatt}). For cases in which the spheres are in set in fixed rather than random orientations, we can calculate the electric field distribution in the near field.

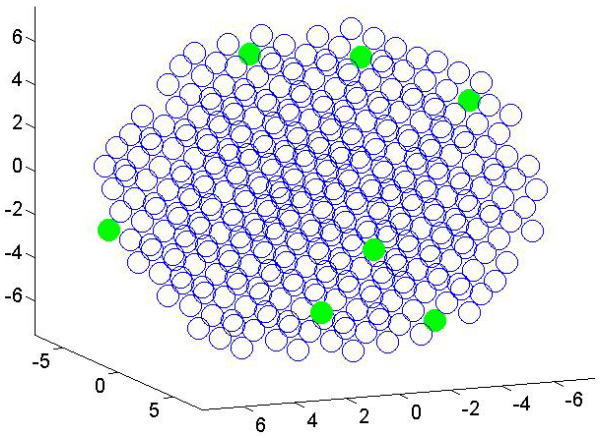

Figure 1. Configuration of the spheres for the Case 2 scattering model. There are a total of 377 spheres (2 um diameter) arranged in cubic close packing configuration. Blue spheres (370) represent halite and green spheres (7) represent olivine.

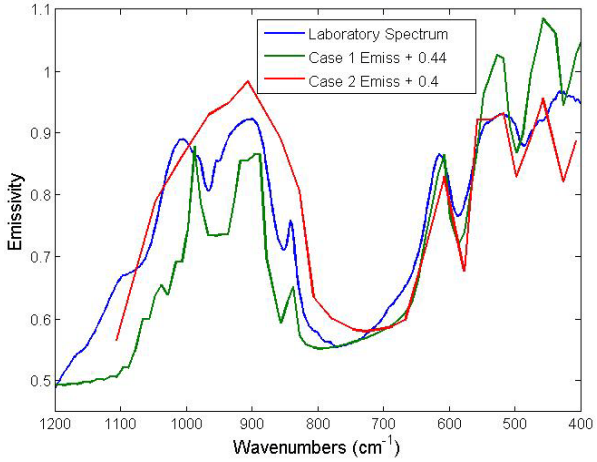

Figure 2. Comparison of measured emissivity spectra and the two model cases described above.

For each wavelength, we calculated the single scattering albedo (w), according to:

$$w = \frac{Q_{scatt}}{Q_{ext}}.$$

We then calculate emissivity according to [11]:

$$\varepsilon = \frac{2\gamma}{1+\gamma}\left(1 + \frac{1}{6}\frac{1-\gamma}{1+\gamma}\right) \text{ where } \gamma = \sqrt{1-w}.$$

For comparison to our calculated emissivity spectra, we used the Stony Brook University Vibrational Spectroscopy Laboratory's emission spectrometer to measure the emissivity spectrum of a mixture of 2% forsteritic olivine in a salt matrix. The mixture was compsed of < 2 μm particles.

Results: The measured and calculated emissivity spectra are shown in Figure 2. Overall, both models reproduce the gross spectral shape of the measured spectrum, although differences are apparent. The Case 1 model includes the calculated emissivities at 80 wavelengths producing ~10 cm^{-1} spectral sampling. Due to the increased calculation time for the larger particle sizes, we were only able to calculate the emissivities at 26 wavelengths for Case 2. For both cases, the overall calculated emissivity was much lower than that of the measured spectrum. For direct comparison to the measured spectrum we were required to add 0.44 and 0.4 emissivity units to the Case 1 and Case 2 models, respectively.

The models also provide insight into the variable photometric properties of surfaces at different wavelengths. Figure 3 shows the normalized scattering phase functions for the Case 2 model at 727 (relatively low k) and 966 (relatively high k) cm^{-1}. For each wavelength, the phase function is 1 to 2 orders of magnitude higher at low phase angle < 10° than at larger phase angles. The normalized phase function at 966 cm^{-1} has generally higher vaules from ~50-180°.

The near-field intensity of the electric field at 906

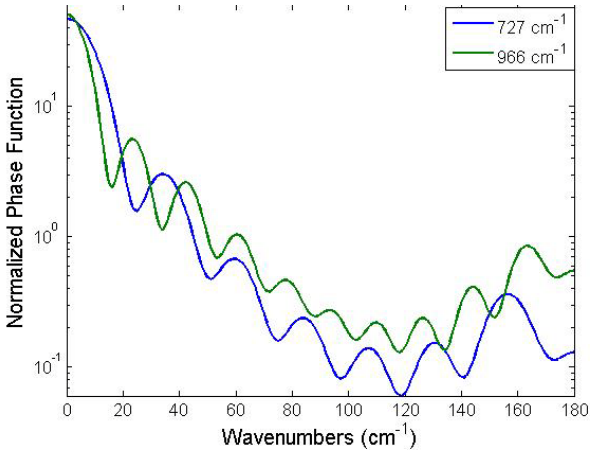

Figure 3. Normalized scattering phase functions for the Case 2 model at 727 (low *k*) and 966 (high *k*) cm^{-1}.

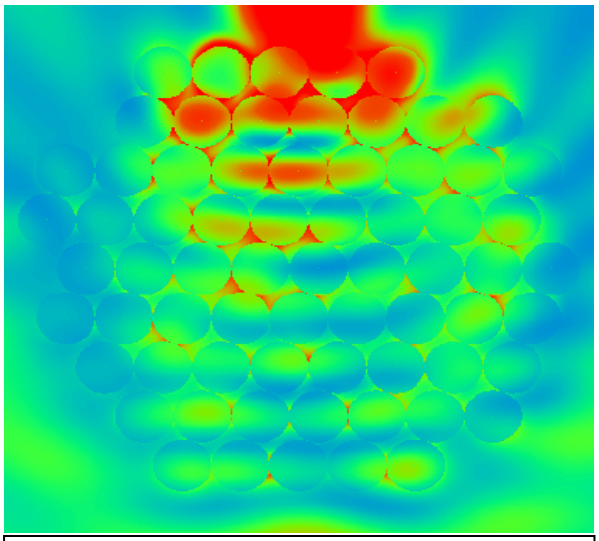

Figure 4. Distribution of the electric field $|E|^2$ for Case 2. The incident beam is at the top of the image. The image is stretched from 0.013 (blue) to 8 (red) V^2/m^2.

cm^{-1} is shown in Figure 4. The incident beam propagates through the medium, although much of the incident beam is attenuated after ~3-4 particle depths. Some scattering is still occurring at 8-9 particle depths, and the field is asymmetric around the cluster surface.

Discussion: While both models reproduce the gross spectral characteristics of our laboratory spectrum, there are still substantial differences between the measured and modeled spectra. There are two likely causes for these differences. The first is the overall size of the modeled volume, which is small relative to the wavelength of the incident radiation. This can be addressed by using a larger volume with more particles, although this can substantially increase the computational time required to solve for the scattering properties at each wavelength. Finally, the distribution of spheres within the cluster obviously affects the scattering characteristics of that cluster. Our future work will focus on determining the optimal particle configuration for studies of regolith surfaces on planetary bodies.

References: [1] Hapke B. (1981) *J. Geophys. Res.*, 86, 3039-3054. [2] Shkuratov Y. et al. (1999) *Icarus*, 137, 235-246. [3] Mishchenko M. I. (2006) *J. Quant. Spec. Rad. Trans.*, 101, 540-555. [4] Mishchenko M. I. (2008) *Rev. Geophys.*, 46, RG2003. [5] Arnold J. A. et al. (2012) *LPS XLIII*, Abstract #2529. [6] Osterloo M. M. et al. (2008) *Science*, 319, 1651-1654. [7] Glotch T. D. et al. (2010) *Geophys. Res. Lett.*, 37, L16202. [8] Jensen H. B. and Glotch T. D. (2011) *J. Geophys. Res.*, 116, E00J03. [9] Yang B. et al. (2012) *Icarus*, in review. [10] Mackowski D. W. and Mishchenko M. I. (2011) *J. Quant. Spec. Rad. Trans.*, 112, 2182-2192. [11] Hapke B. W. (1993b) Cambridge Univ. Press, New York.